Article

Journal of Nanoscience and Nanotechnology
Vol. 14, 9143–9147, 2014
www.aspbs.com/jnn

Aerosol Approach for Hollow Spheres of a Porous 3D Carbon Nanotube/CuO Network and Their Anodic Properties for Lithium-Ion Battery

YunKyoung Kim[1], SeungIl Cha[2], JunHo Lee[1], and SoonHyung Hong[1,*]

[1] *Department of Materials Science and Engineering, Korea Advanced Institute of Science and Technology, Daejeon, 305-701, Republic of Korea*
[2] *Advanced Materials and Application Research Division, Korea Electrotechnology Research Institute, Changwon, 641-120, Republic of Korea*

Hollow spheres consisting of porous CNT/CuO nanocomposite networks were prepared by aerosol process and their enhanced anodic properties for lithium-ion battery were investigated. Hollow spheres of CNT/CuO nanocomposites showed a 3D network wherein the length of the electron path was quite short compared with the agglomerated CNT/CuO nanocomposites. From electrochemical measurements, CuO itself shows poor discharge capacity and cycling performance due to its low electronic conductivity. In the CNT/CuO nanocomposite, enhanced discharge capacity was observed and showed similar values regardless of the morphology. With the addition of CNTs to CuO, CNTs can form a network that acts as an electron path-way in the insulating CuO matrix, leading to increased electrical conductivity. The morphology of nanocomposite affected cycle stability. Hollow spheres of CNT/CuO nanocomposite showed better cycle stability than that of agglomerated CNT/CuO nanocomposite. The hollow sphere of a CNT/CuO nanocomposite comprising a 3D network of CNTs can be applied as a high capacity anode material in Li-ion batteries.

Keywords: Carbon Nanotubes, Nanocomposite, Lithium-Ion Battery.

1. INTRODUCTION

Lithium-ion batteries have become the dominant power sources for portable electronic devices.[1] These batteries are also expected to be widely used for the power supply in hybrid electric vehicles (HEVs) and electric vehicles (EVs). Due to demand for higher energy storage for new applications, huge efforts have been made to develop new electrode materials for lithium-ion batteries with improved electrochemical properties.

Recently, transition metal oxides have been studied as anode materials of lithium-ion batteries. The use of transition metal oxides as electrode materials for next generation rechargeable lithium-ion batteries with both high energy and high power densities have been widely studied owing to their high theoretical capacity, high safety, environmental benignity, low cost, etc.[2] Transition metal oxides operate by a mechanism based on a process termed the conversion reaction. The reaction leads to the formation of nanosized metal particles and amorphous Li_2O, via a reversible process, and the associated lithium storage capacity can be maintained for hundreds of cycles. Among these transition metal oxides, CuO could be an attractive anode material because it is inexpensive, non-toxic, easily produced, readily stored and has a high theoretic capacity (670 mA h g^{-1}). However, the conversion reactions suffer from poor kinetics, leading to low cycle performance. One of the challenging issues related to their use for high performance lithium-ion batteries is tackling their poor electronic conductivities. Research has focused on enhancing electronic conduction by using carbon-coatings[3,4] or other electronically conductive additives.[5,6] Carbon nanotubes (CNTs) are attractive materials for energy storage applications such as supercapacitors, fuel cells, and lithium-ion batteries due to their high chemical stability, high aspect ratio, and excellent mechanical, electrical, and thermal properties.[7] In particular, it has been reported that the specific capacity of Li-ion battery can be improved by the superior electric conductivity of

*Author to whom correspondence should be addressed.

CNT/metal oxide nanocomposites.[8] Guo et al. synthesized CuO-CNT composites by self-assembly, and CuO-CNT composite spheres exhibited remarkably enhanced cycling performance and rate performance compared with CuO spheres when used as anode materials in lithium-ion batteries.[8] Wang et al. fabricated CNT/Co oxide core-shell one-dimensional nanostructures by a hydrothermal synthesis method, wherein nanosize cobalt oxide crystals were homogeneously coated on the surface of carbon nanotubes and showed initial lithium storage capacity of 1250 mA h g^{-1} and a stable capacity of 530 mA h g^{-1} over 100 cycles.[9] Grugeon et al. reported on the electrochemical reactivity of tailor-made Cu_2O or CuO powders prepared by a polyol process and showed that the ability of copper oxide-based Li cells to retain their capacity upon numerous cycles was strongly dependent on the particle size.[10] However, the proper design for a CNT/metal oxide system in order to obtain promising electrochemical performance has not been reported.

In this paper, we report on a hollow sphere of porous CNT/CuO nanocomposite, prepared by spray drying process, as an anode material for lithium-ion batteries. For comparison, agglomerated CNT/CuO nanocomposite particles and hollow spheres of CuO nanoparticles were prepared by a solvent evaporation process and a spray dry method and their electrochemical properties were systematically tested. The improved electrochemical performance of hollow sphere of CNT/CuO nanocomposite networks as anode materials in lithium-ion cells are ascribed to the enhanced electrical conductivity due to the addition of carbon nanotubes and higher exposed surface area to the electrolyte.

2. EXPERIMENTAL DETAILS

CuO and CNT/CuO nanocomposites were fabricated by two different methods. Agglomerated CNT/CuO nanocomposite particles were prepared by a solvent evaporation process, and hollow spheres of a CNT/CuO nanocomposite were obtained by an aerosol approach. CuO and CNT/CuO nanocomposite was synthesized by calcinations of Copper(II) acetate monohydrate (CuAc, $Cu(CO_2CH_3)_2 \geq 98\%$, Aldrich) and CNT/CuAc nanocomposite which fabricated by both solvent evaporation process and spray drying. In solvent evaporation process, CuO was synthesized by calcinations of CuAc which used as the Cu source. CNTs (CM95, Hanwha Nanotech) were purified and functionalized by acid treatment using H_2SO_4 and HNO_3. The CNTs were ultrasonicated in mixed solution of H_2SO_4/HNO_3 in a 3:1 ratio and washed with D.I. water. Functionalized CNTs and Cu salts were each dispersed in ethanol and mixed up by ultrasonication. CNT/CuAc nanocomposite was synthesized by heating mixtures over 80 °C for all solvents evaporated. In spray dry process, CuAc and mixture of functionalized CNT and CuAc solution was spray dried by using spray dryer (SD-1000, EYELA). The spray drying conditions in the preparation of CuO and CNT/CuO nanocomposite particles were as follows: the sample feeding rate was 25 mL min^{-1}, highly pressurized air was 150 kPa, and the hot airflow rate was 0.15 m^3 min^{-1}; the inlet and outlet temperatures of the drying chamber were at 120 °C and 68 °C, respectively. CuAc and CNT/CuAc nanocomposite fabricated by solvent evaporation process and spray drying both converted to CNT/CuO nanocomposite by calcinations at 400 °C, 1 hr in air. The prepared CuO and CNT/CuO was characterized by X-ray diffraction (D/MAX-IIIC, RIGAKU) and morphology was examined by scanning electron microscopy (S-4800, HITACHI).

Electrochemical measurement was performed by automatic battery cycler system (WBCS 3000, WonATech), using 2014 coin type cell. The CuO and CNT/CuO nanocomposite powders were mixed with 20 wt.% acetylene black and 10 wt.% poly-vinylidenedifluoride (PVDF) binder in *N*-methylpyrrolidone (NMP) solvent. The electrode mixture was spread on Copper foil. The electrolyte was 1 M $LiPF_6$ in a mixture (1:1 vol. ratio) of ethylene carbonate (EC) and dimethyl carbonate (DMC). The cycling was performed at rate of 0.1 C, over a voltage range of 0.01–3.0 V versus a Li/Li^+ counter electrode. All specific capacities were calculated by mass of composite material.

3. RESULTS AND DISCUSSION

Initially, we designed two types of CNT/CuO nanocomposites, agglomerated CuO nanoparticles and a 3D network of CNTs and CuO nanoparticles, as indicated in Figure 1. The agglomerated CuO nanoparticles are expected to have low electrical conductivity due to having a long electron path. The conductivity can be improved by using CNTs to provide electron paths in the CNT/CuO nanocomposite. However, the electron path might also be long if the CNT/CuO nanoparticles have an agglomerated

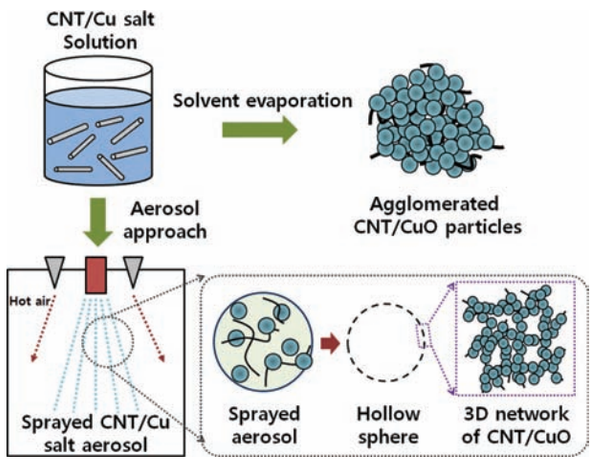

Figure 1. Schematic illustration for fabrication of CNT/CuO nanocomposite particles and hollow sphere of CNT/CuO nanocomposite.

form. In the 3D network of the CNT/CuO nanocomposite, electrons easily access to CNTs due to the homogeneous dispersion of CNTs as well as the reduced distance between CNTs and CuO nanoparticles. Therefore, the 3D networked CNT/CuO nanocomposites are expected to show superior electrochemical performance.

CuO and CNT/CuO nanocomposites were fabricated by two different methods. Agglomerated CNT/CuO nanocomposite particles were prepared by a solvent evaporation process, and hollow spheres of a CNT/CuO nanocomposite were obtained by an aerosol approach. Their microstructures are shown in Figure 2. For the agglomerated CNT/CuO nanocomposite, the particle size of CuO was found to be approximately 20 nm was quite similar between CuO and the CNT/CuO nanocomposite. CNTs were well dispersed and homogeneously implanted in the CuO particles. However, serious agglomeration of CuO nanoparticles was observed in pure CuO and the CNT/CuO nanocomposites. Hollow spheres of CuO and CNT/CuO nanocomposite showed a porous surface and the average size of the CuO spheres was 2 μm. In particular, the CNT/CuO nanocomposites showed a network formed by CNTs, which were covered with CuO nanoparticles, as seen in the SEM images of Figure 2(f).

The phase of the cupper oxide was confirmed by the X-ray diffraction analysis. When the precursor was calcined above 400 °C, 1 hr in air, the black CuO powders were obtained. Figure 3 shows the XRD patterns of the nanoparticles synthesized in this study and all the three types of the samples were exhibited same XRD patterns.

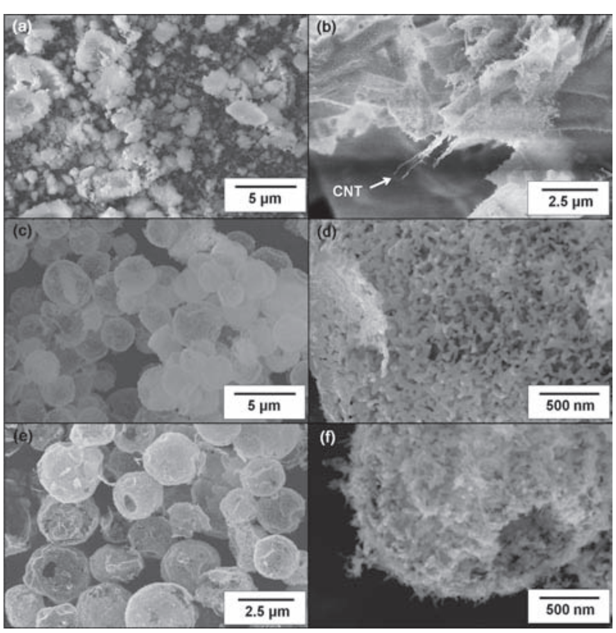

Figure 2. SEM images of pure CuO and CNT/CuO nanocomposites: (a) pure CuO prepared by solvent evaporation process, (b) solvent-evaporated CNT/CuO nanocomposite, (c), (d) spray dried CuO and (e), (f) spray dried CNT/CuO nanocomposite.

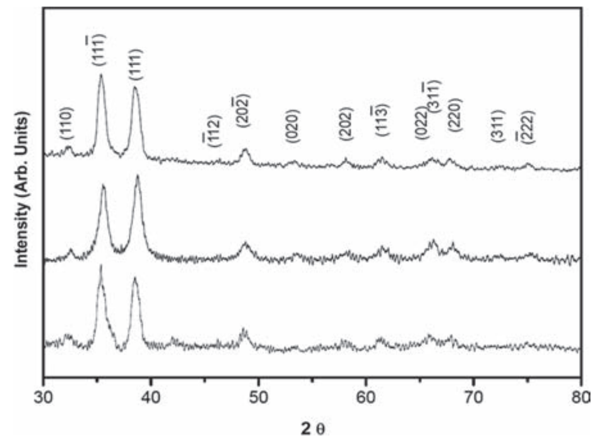

Figure 3. XRD patterns of pure CuO and CNT/CuO nanocomposites.

As seen in Figure 3, all the peaks were indexed to CuO phase and any other peak was not detected.

Thus, it could be said that CuO was well-synthesized at all the three types of pure CuO and CNT/CuO nanocomposites. Therefore, we could conclude that the designed nanostructures were well-synthesized and superior electrochemical performance might be observed in hollow spheres of CNT/CuO nanocomposite.

Electrochemical properties of CuO and CNT/CuO nanocomposite as anode materials in Li-ion cells were evaluated by charge–discharge cycling tests. The cycling was performed at rate of 0.1 C, over a voltage range of 0.01–3.0 V versus a Li/Li^+ counter electrode. For all four types of material, the potential falls rapidly to reach a large plateau at 1.3 V, and then slowly drops to 0.01 V in the first discharge, as shown in Figure 4. For CuO fabricated by a solvent evaporation process, the discharge capacity of lithium ions upon the first discharge reached 480 mA h g^{-1} and the subsequent charge capacity amounted to 162 mA h g^{-1}, which is similar to the value of the second discharge capacity, 167 mA h g^{-1}. In the case of spray dried CuO, the discharge capacity was 727 mA h g^{-1} on the first discharge and the charge capacity was 203.8 mA h g^{-1}. Both CNT/CuO nanocomposite materials, that is, agglomerated CNT/CuO nanocomposite and hollow sphere of CNT/CuO nanocomposite, showed enhanced capacity. For the agglomerated CNT/CuO nanocomposite, the first discharge capacity reached 733 mA h g^{-1} and the charge capacity reached 264 mA h g^{-1}. Spherical CNT/CuO nanocomposite fabricated by the aerosol approach showed 947 mA h g^{-1} for the first discharge capacity and 289 mA h g^{-1} for the charge capacity. The charge capacity of the CNT/CuO nanocomposite was enhanced 1.7 times relative to that of CuO, and showed similar values regardless of the fabrication process. This is evidence that the capacity was enhanced due to the incorporation of the CNTs. With the addition of CNTs to CuO, CNTs form a network and provide effective pathways for electrons in the insulating CuO

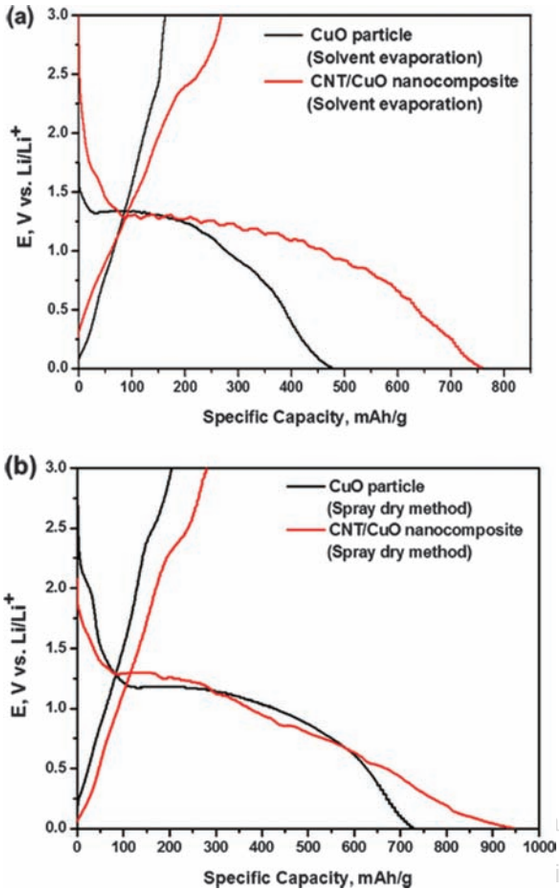

Figure 4. Charge/discharge curves of (a) CuO particle, CNT/CuO nanocomposite prepared by solvent evaporation and (b) CuO particle, CNT/CuO nanocomposite fabricated by spray dry method.

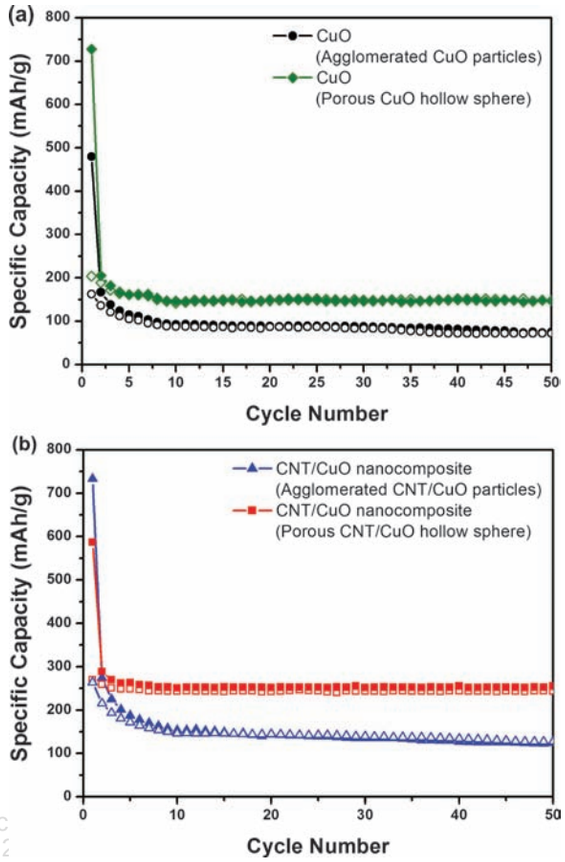

Figure 5. Cycle retention of (a) pure CuO and (b) CNT/CuO nanocomposites.

matrix, leading to increased electrical conductivity. Therefore, the enhanced discharge capacity can be explained by the higher electrical conductivity of the CNT/CuO nanocomposite.

For characterization of cycle performance, charge–discharge tests of cells were performed for 50 cycles. After 50 cycles, the capacity remains at around 71 mA h g^{-1}, which is 42.5 % of the initial second discharge capacity for CuO synthesized by the solvent evaporation process, and 147 mA h g^{-1}, which is 72% of the initial second discharge capacity for hollow sphere of CuO. In the case of the agglomerated CNT/CuO nanocomposite, the capacity remains at 124 mA h g^{-1} after 50 cycles, 47% of the initial second discharge capacity. For the hollow sphere of CNT/CuO nanocomposite, the capacity remains at 243 mA h g^{-1} after 50 cycles, 84% of the initial second discharge capacity. As shown in Figure 5, the cycle performance of CuO and the CNT/CuO nanocomposite show difference by their preparation method. Capacity retention of CuO hollow sphere was similar to that of the CNT/CuO nanocomposite fabricated by the aerosol approach, showing good stability. This could be explained by the formation of a SEI layer on the active material during charge–discharge cycling. The growth of an organic layer resulting from the reaction of the solvent electrolyte molecules at the surface of metallic nanograins is a well-known phenomenon.[8] This coated polymer layers ensure better mechanical contact between highly divided grains; however, in nanosized active materials, it could cause detachment of the conductive agent and negatively affect the electrode capacity retention upon cycling.

4. CONCLUSIONS

In summary, CuO and CNT/CuO nanocomposites were fabricated by a solvent evaporation process and aerosol approach. By using functionalized CNTs, CNTs were well dispersed and homogeneously implanted in CuO particles. CuO and CNT/CuO nanocomposites have shown different size and morphology according to the fabrication process. The CNT/CuO nanocomposite prepared by an aerosol approach showed porous hollow spherical CuO and CNTs formed a 3D network with CuO nanoparticles. From electrochemical measurement, pure CuO displayed poor discharge capacity and cycling performance, which are attributed to its low electronic conductivity. In the

CNT/CuO nanocomposite, the second discharge capacity was enhanced 1.7 times relative to that of CuO, and similar values were obtained regardless of the fabrication process. Enhanced discharge capacity was observed with the addition of CNTs to CuO, and is ascribed to increased electrical conductivity. With the addition of CNTs to CuO, CNTs can form a network that acts as an electron pathway in the insulating CuO matrix, leading to increased electrical conductivity. The morphology and size of CuO affected the cycle stability of the electrode. Hollow spheres of CuO and the CNT/CuO nanocomposite showed better cycle stability than the agglomerated CuO and CNT/CuO nanocomposite. This could be explained by a particle size effect due to the formation of a SEI layer on the active material during charge–discharge cycling. The amorphous SEI layer coating negatively affects the electrode capacity retention upon cycling. The results here provide clear evidence of the utility of dual functional CNTs to improve the electrochemical performance of transition metal oxides as electrode materials for lithium-ion batteries. The strategy is simple, yet very effective, and on the basis of its versatility it could also be extended to other anode materials used in lithium-ion batteries.

Acknowledgments: This work was supported by Priority Research Centers Program through the National Research Foundation of Korea (NRF) funded by the Ministry of Education, Science and Technology (2011-0031407).

References and Notes

1. J. M. Tarascon and M. Armand, *Nature* 414, 359 (**2001**).
2. F. Jiao and P. G. Bruce, *Adv. Mater.* 19, 657 (**2007**).
3. G. Derrien, J. Hassoun, S. Panero, and B. Scrosati, *Adv. Mater.* 19, 2336 (**2007**).
4. S. H. Ng, J. Z. Wang, D. Wexler, K. Konstantinov, Z. P. Guo, and H. K. Liu, *Angew. Chem. Int. Edit.* 45, 6896 (**2006**).
5. L. Kavan, I. Exnar, J. Cech, and M. Graetzel, *Chem. Mater.* 19, 4716 (**2007**).
6. F. Badway, A. N. Mansour, N. Pereira, J. F. Al-Sharab, F. Cosandey, I. Plitz, and G. G. Amatucci, *Chem. Mater.* 19, 4129 (**2007**).
7. S. Iijima, *Nature* 354, 56 (**1991**).
8. S. F. Zheng, J. S. Hu, L. S. Zhong, W. G. Song, L. J. Wan, and Y. G. Guo, *Chem. Mater.* 20, 3617 (**2008**).
9. G. Wang, X. Shen, J. Yao, D. Wexler, and J. H. Ahn, *Electrochem. Commun.* 11, 546 (**2009**).
10. S. Grugeon, S. Laruelle, R. Herrera-Urbina, L. Dupont, P. Poizot, and J. M. Tarascona, *J. Electrochem. Soc.* 148, A285 (**2001**).

Received: 8 April 2013. Accepted: 10 December 2013.